EUROPEAN ORGANIZATION FOR NUCLEAR RESEARCH
European Laboratory for Particle Physics

Internal NOTE

ALICE reference number

ALICE-INT-2009-029 version 1.0

Date of last change

November, 2009

Measurement of pseudorapidity density of charged particles in proton-proton collisions with the ALICE Pixel detector

D. Elia[a], B. Ghidini[b] and M. Nicassio[a]

a. Sezione INFN, Bari, Italy

b. Dipartimento Interateneo di Fisica "M. Merlin" and Sezione INFN, Bari, Italy

Abstract

This note describes a procedure for measuring the pseudorapidity density distribution of charged particles, based on the tracklets reconstructed with the silicon pixel layers. Results on proton-proton Monte Carlo samples are presented.

1 Introduction

The aim of this note is to describe a procedure to measure the pseudorapidity (η) density distribution of primary charged particles produced in proton-proton collisions. The method is based on reconstructed pseudo-tracks (tracklets) obtained using the information provided by the Silicon Pixel Detector (SPD) [1] only. It takes into account the number of events and several correction factors to get from the reconstructed to the physical distribution. An alternative method has been developed and described in Ref. [2]: the main difference with respect to the method presented here is that a global correction factor for all the effects is considered there.

The pseudorapidity density distribution in proton-proton collisions will be the first measurement carried out with the ALICE detector, first at a centre of mass energy of $\sqrt{s}$ = 900 GeV (LHC injection energy) and then at $\sqrt{s}$ = 7 and 10 TeV along the first year of data taking. The measurements at low energy will be compared with the existing measurements for $p - \bar{p}$ collisions at the same centre-of-mass energy at S$p\overline{p}$S: among the other things, this will allow a global check of the systematics. The following measurements up to $\sqrt{s}$ of 14 TeV will allow to extend the energy dependence range and enter the realm of the new physics with LHC. Both for proton-proton and heavy-ion collisions this measurement has a key role in the global event characterization: it will allow to constrain the hadroproduction models, correctly configure the Monte Carlo generators and determine the energy dependence of the charged-particle density.

In ALICE the reconstruction of the pseudorapidity density distribution in the central η region can be performed using data provided by the SPD only, that consitutes the two innermost layers of the Inner Tracking System (ITS) [3]. The two SPD layers are equipped with silicon pixels: their average distances from the beam line are 3.9 and 7.6 cm and they cover pseudorapidity acceptance regions $|\eta| < 2$ and $|\eta| < 1.4$ respectively, as defined for particles originating at the centre of the detector. Compared to the corresponding measurement based on the tracks reconstructed with the ITS and the Time Projection chamber (TPC) or with the TPC only, the multiplicity reconstructed with pixels has some basic advantages: a larger acceptance coverage both in pseudorapidity and in p_T (down to 30 MeV/c) and a much smaller reliance on the alignment and calibration procedures [4, 5]. The last aspect turns out to be crucial since will allow to extract results from the very first available data.

The note is organized as follows. In Section 2 the reconstruction procedure will be briefly described. In Section 3 the Monte Carlo samples used in this analysis will be listed and the event selection criteria will be summarized. In Section 4 and 5 the method and

the corrections will be discussed, then applied to the Monte Carlo samples as described in Section 6.

2 Reconstruction procedure

A detailed description of the tracklet reconstruction algorithm and its performance can be found in Ref. [6]. The algorithm needs the reconstructed points (clusters[1]) of the SPD and the reconstructed main vertex position as input. The primary vertex is reconstructed using SPD clusters as well, as explained afterwards.

Using the reconstructed vertex as the origin, the algorithm calculates the differences in the azimuthal angles ($\Delta\varphi$) and in the polar angles ($\Delta\theta$) between a cluster in the inner layer and each cluster in the outer layer. An elliptical cut is applied (sum of the squares of $\Delta\varphi$ and $\Delta\theta$ each normalized to its estimated resolution, $\Delta\varphi_{cut}$ and $\Delta\theta_{cut}$ respetively) and for the cluster in the outer layer that matches the cluster in the inner layer with the shortest distance, a list of the matching clusters in the inner layer and the corresponding distances is made. This procedure is performed for each cluster in the inner layer. At the end of the loop over clusters in the inner layer, the pairs associated are labelled and saved as "tracklets". A decision is made for clusters in the outer layer that have more than one cluster in the inner layer in their partner list: they are associated to the one with the minimum distance. This procedure garantees that only pairs with the minimum distance are associated over all the possible combinations, independently of the cluster order. Once associated to build a tracklet, clusters are removed from the list of the available clusters and these steps are iterated using all the remaining clusters from the previous step. The iteration stops where no more associations are found.

The cuts used by default in the reconstruction are $\Delta\varphi_{cut} = 0.08$ rad and $\Delta\theta_{cut} = 0.025$ rad respectively. The cut imposed in the azimuthal angle corresponds to a transverse-momentum cut-off of about 35 MeV/c. The efficiency in reconstructing primary particles is about 98% and the backgound percentage (tracklets made up of clusters produced by secondary particles and combinatorics) is about 5%. Since the variables on which the cuts are applied are stored in the ESD file for each tracklet, tighter cuts can be applied at the analysis level, provided the new cuts scale both proportionally with respect to the default cuts. The pseudorapidity η is evaluated by considering a straight line from the main vertex to the position of the cluster in the inner layer (since better measured). The multiplicity of charged particles is estimated counting the number of tracklets. The tracklet-based method for multiplicity studies is a proven technique used in the PHOBOS experiment

[1] A cluster is made up of one or more hit adjacent pixels.

at RHIC [9] and, in general, allows a good rejection of the background (detector noise, secondary particles, residual beam-gas contamination).

3 Analysis samples and event selection

The results that will be shown in this note have been obtained using the First Physics official Monte Carlo productions of the Physics Data Challenge 2009 (PDC09) available on the CERN Analysis Facility (CAF) and produced with the most updated version of the simulation and reconstruction code. In particular the following minimum-bias p-p samples at $\sqrt{s} = 7$ TeV have been employed to compute the corrections and some of the associated systematic errors:

- 275000 Pythia events with magnetic field B = 0 T;
- 59000 Pythia events with magnetic field B = 0.5 T.
- 175000 PhoJet events with magnetic field B = 0 T;
- 21700 PhoJet events with magnetic field B = 0.5 T.

All the results that will be shown in the next sections will refer to the last sample in the list, unless otherwise specified. All these samples have been reconstructed considering a given map of dead pixels (in the real case corresponding to disconnected and/or noisy parts of the detector). This maps consists of the following parts: known dead pixels since detector construction (6488 pixels), one half of a chip (4096 pixels) and 15 half staves (6 in the inner layer and 9 in the outer layer). This distribution makes up the 13% of the SPD: 10% in side A and 15% in side C, hence it is not symmetric in η. This appears clearly in the plots of the cluster occupancy for both the SPD layers shown in Fig. 1.

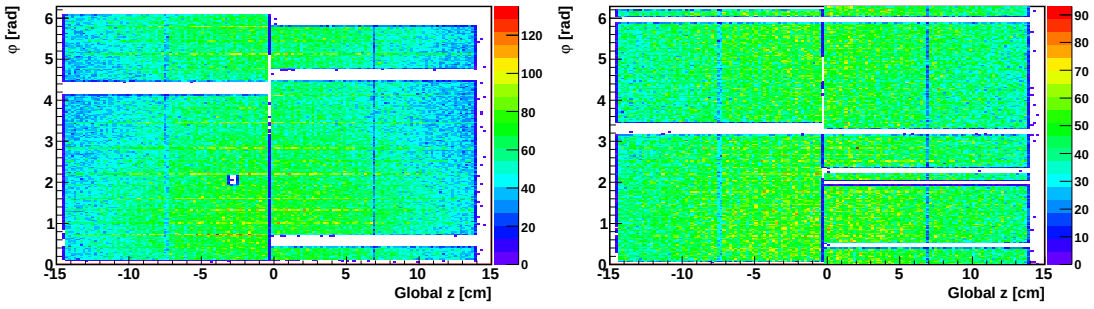

Figure 1: *Cluster maps for the inner (left panel) and the outer layer (right panel) of the SPD, with the dead pixel map assumed in the PDC09 Monte Carlo samples.*

Events usable for the analysis are selected in two phases: the trigger selection and the analysis level selection. A minimum bias trigger will be applied in the data acquisition: for p-p events this selection will be performed exploiting the capability of both the VZERO detector signals and the SPD Fast-Or [1]. Combinations of the two detector signals are expected to be able to select inelastic collisions with very high efficiency, rejecting almost all the events coming from collisions of the proton beam with the residual gas in the beam pipe (beam-gas interactions) [10]. The two most efficient algorithms, MB1 and MB2, are based on the following conditions:

$$\texttt{MB1} \equiv \texttt{(V0OR).or.(GlobalFO).and.notBG}$$
$$\texttt{MB2} \equiv \texttt{(V0OR).and.(GlobalFO).and.notBG}$$

The presence of at least a Fast-Or signal in the whole SPD (GlobalFO) or/and at least one hit on either one of the two V0 scintillators arrays at a time of a beam-beam interaction (V0OR) are required. The condition `notBG` allows to reject beam-gas events: it is a veto signal from the V0 detector based on the definition of time windows around the time corresponding to beam-gas interactions. In Tab. 1 the efficiencies for the two MB trigger algorithms and for different event classes are reported, while in the left panel of Fig. 2 the MB1 trigger efficiency is shown as a function of the generated Monte Carlo multiplicity.

	Efficiency (%)			
Event type	Inelastic	ND	SD	DD
MB1	95.5	99.9	72.7	89.6
MB2	91.2	99.2	56.4	69.0

Table 1: *Efficiencies for the MB1 and MB2 trigger algorithms for different event classes. The percentages are quoted for the assumed distribution of the SPD dead channels (about 13%).*

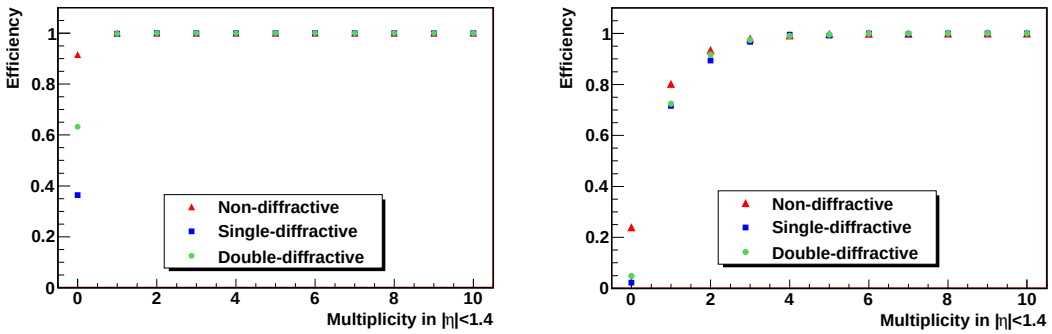

Figure 2: *Efficiency of the MB1 trigger (left panel) and vertex reconstruction in triggered events as as a function of the multiplicity for different event classes (right panel).*

In the following the MB1 trigger algorithm is used to select events. A trigger condition equivalent to the one described will be applied to data offline; however, a constant rate trigger will be applied for first data-taking, based on bunch-crossing signals.

A further selection is performed at level of reconstruction and analysis, since triggered events usable to build tracklets must have the primary vertex reconstructed: the vertex position cannot be assumed known, as it will have a spread around the nominal interaction point. Indeed the proton beams will have a nominal spread: the LHC machine parameters at the ALICE intersection point for p-p beams at 450 GeV/c momenta are $\sigma_{x,y}^{vertex} \approx 270\ \mu m$ and $\sigma_{z}^{vertex} \approx 7.09\ cm$ in the transverse plane and in the beam direction respectively [12]. The position of the primary vertex used in the present analysis has been reconstructed exploiting the correlation between the clusters in both the SPD layers as described in [7, 8]. For p-p events the algorithm tries to find the three coordinates of the primary vertex. If it fails, an algorithm that tries to calculate the z-coordinate only is called. The resolution depends on the track multiplicity and is about 0.1-0.3 mm in the longitudinal direction and 0.2-0.5 mm in the transvers directions. The efficiency as a function of the Monte Carlo multiplicity in $|\eta|$ <1.4 for triggered events is shown in the right panel of Fig. 2.

In the analysis only events with the z coordinate of the reconstructed vertex $|z_{SPDvtx}| <$ 10 cm will be used, since the efficiency and reliability decreases for larger values. Events usable for the tracklet reconstruction and subsequently for the analysis are those selected by the trigger that have the primary vertex reconstructed. The measured distributions have to be properly corrected to take into account the bias produced with these selections on the sample analized.

4 Method description

The reconstructed distribution has to be corrected for several effects to obtain the physical distribution of primary charged particles. Primary particles are defined as particles produced by the event generator and the products of electromagnetic and strong decays. The products of weak decays and particles from feed-down are excluded. Two event classes will be considered in this study: inelastic and non-single diffractive events. The following effects in the reconstructed distribution will be considered:

- background from secondary particles;
- algorithm and detector inefficiency;
- detector acceptance;

- particles that do not reach the sensitive layers of the detector;
- vertex reconstruction inefficiency;
- minimum bias trigger inefficiency.

These effects and the corresponding corrections have been studied both at tracklet and at event level. To calculate them, information from both reconstruction and Monte Carlo is needed. The reconstructed data are stored in two-dimensional histograms at track and event level. Two classes of events are considered for data and consequently in the correction calculation: triggered events and triggered events in which a vertex has been found. In the latter only events with the z-coordinated of the reconstructed vertex in $|z_{SPDvtx}|$ <10 cm and at least one tracklet reconstructed $mult_{SPD} > 0$ are considered (reconstructed events in the following). The two additional conditions garantees that the vertex determination is reliable. Reconstructed events will be indicated in the text as trigVtxEvts and triggered events as trigEvts. One histogram to apply corrections tracklet by tracklet is filled for each reconstructed event with the reconstructed vertex position z_{SPDvtx} and the pseudorapidity η_{SPD} of each tracklet

$$tracklets(\eta_{SPD}, z_{SPDvtx}) \tag{1}$$

At event level two histograms are filled with the reconstructed vertex and the tracklet multiplicity for the proper event class:

$$triggVtxEvts(mult_{SPD}, z_{SPDvtx}) \tag{2}$$

$$triggEvts(mult_{SPD}, z_{SPDvtx}) \tag{3}$$

one for reconstructed events and the other for triggered events only. The zero-multiplicity bin will be empty for the first histograms since these events are not considered in the definition of that event class and, for the second one, will be always filled with $z_{SPDvtx} =$ 0 cm since, even if determined, this value is not considered reliable. The three histograms above mentioned can be filled in both for real and simulated events and will be used to apply corrections at event level to calculate then the correct normalization factors for the corrected $dN_{ch}/d\eta$ distributions. For the simulated events only, two-dimensional histograms are used to store the multiplicative factors for corrections both at tracklet level and event level respectively:

$$TLC_i(\eta, z_{vtx}) \qquad\qquad ELC_i(mult_{SPD}, z_{MCvtx}) \tag{4}$$

The data and the correction histograms have the same binning that can be set appropriately. The products of data matrices and corrections are stored in independent histograms

to have the result at each correction step. The pseudorapidity distributions are obtained from the projection of these products histograms on the η axis. The dN/dη distributions will result from the ratio of the the pseudorapidity distributions and the proper normalization histograms or factors that will be described later. Therefore the final distribution in each pseudorapidity bin is given by

$$\frac{dN}{d\eta}(\eta) = \frac{\int_z tracklets(\eta, z) * \prod_i TLC_i(\eta, z)\, dz}{\int_{z_1}^{z_2} \sum_{mult} triggVtxEvts(mult, z) * triggEvts(mult, z) * \prod_j ELC_j(mult, z)\, dz} \tag{5}$$

where z_1 and z_2 are the minimum and the maximum values of the vertex position that gives that η value in the SPD acceptance. Finally, the number of pseudorapidity bins per unit of pseudorapidity multiplies the content of each bin. The products over the corrections can be limited to a subset of corrections to obtain the distribution at each step of the correction process.

5 Corrections

In this paragraph the corrections and their calculation method will be described. The result for each correction will be also shown.

5.1 Track level corrections

The corrections at track level are calculated as a function of the pseudorapidity η and the z-coordinate of the primary vertex and are stored in two-dimensional histograms. The binning of those histogram is 2 cm in z and 0.1 in η. The corrections needed at track level are the following:

- background from secondary particles;
- algorithm and detector inefficiency;
- detector acceptance;
- particles that do not reach the sensitive layers;
- vertex reconstruction inefficiency;
- minimum bias trigger inefficiency.

To calculate them, the following information produced in the reconstruction is retrieved from the ESDs files:

- the reconstructed vertex position z_{SPDvtx}

- the tracklet pseudorapidity η_{SPD}
- the two Monte Carlo particle labels of the clusters in the tracklet.

Furthermore the following Monte Carlo variables allow to complete the calculation:

- the vertex position z_{MCvtx};
- the pseudorapidity η_{MC} of primary particles;
- particle indeces;
- the track references produced during particle trasport through the detector;
- the event type.

Using all those information, the generated primary particles can be subdivided into the following subsets:

- **reconstructed**: primaries that have a tracklet associated;
- **reconstructable**: primaries that might produce at least one pair of cluster (one in each layer);
- **detectable**: primaries crossing the two SPD layers.

Background from secondaries Because of the presence of particles produced in secondary interactions and decays, a certain amount of background tracklets will be reconstructed, that is tracklets that cannot be associated to a primary particle: pairs of clusters produced either by two different particles (combinatorics) or by the same secondary particle can be associated each other. A correction factor is needed for background subtraction.

Background tracklets have been identified by means of the labels each cluster has that record the particle or particles that generated it. Each cluster has at most three labels and for each tracklet two labels are stored: if the two clusters associated have at least one equal label, the tracklet takes that label for each of the two clusters, otherwise the first label for each cluster is stored. These labels allow to select primaries that have been reconstructed: for each primary if a tracklet is found having both labels matching with this primary, it is labeled as **reconstructed**. For each reconstructed primary particle a two dimensional histogram is filled using the values of the generated pseudorapidity η_{MC} and the generated vertex position z_{MCvtx}. For each reconstructed tracklets, both primary and background tracklets, another two dimensional histogram is filled with reconstructed pseudorapidity η_{SPD} and the reconstructed vertex position z_{SPDvtx}. The correction is the

ratio between the two histograms and is shown in Fig. 3:

$$TC_{Bkg}(\eta, z_{vtx}) = \frac{\sum_{triggVtxEvts} \#reconstructedPrimaries(\eta_{MC}, z_{MCvtx})}{\sum_{triggVtxEvts} \#tracklets(\eta_{rec}, z_{SPDvtx})} \quad (6)$$

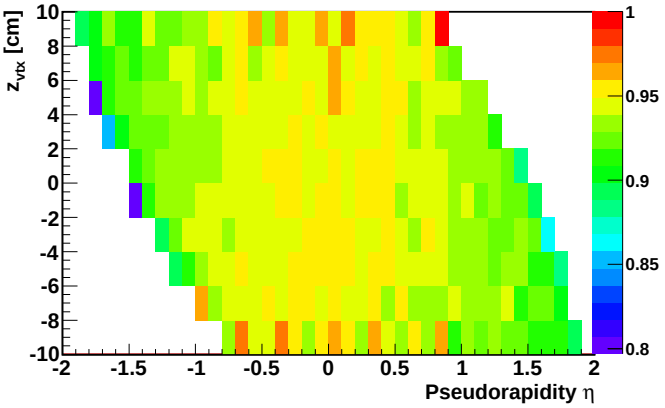

Figure 3: *Background correction: ratio between the reconstructed primaries and all the reconstructed tracklets for each bin.*

The background fraction is about 6% in the central pseudorapidity region and increases up to 10% with the pseudorapidity due to the longer distance and the amount of material budget crossed. This correction will depend on the cuts applied in the reconstruction: the larger the windows, the higher the background fraction. The cuts for the tracklet reconstruction have to balance the background fraction and the reconstruction efficiency. However a lower background percentage than higher efficiency is advisable as, in principle, the background might depend on the multiplicity, while, on the other hand, the correction for the tracklet algorithm inefficiency only depends on the cut window widths. The overall background fraction with the default cuts used in tracklet reconstruction is about 5%.

Tracklets reconstruction inefficiency The algorithm is inefficient if it fails to associate a pair of clusters produced by the same primary particle in each the two SPD layers. Two effects can cause the failure: either the wrong association of the cluster in the outer layer to make up a combinatoric tracklet or the width of the fiducial window.

All the primaries producing at least one cluster on both the SPD layers should be defined as **reconstructable** primaries. However, since the clusters are not available in the ESDs, the track references are used for this purpose. For most of the detectors, for each primary particle a track reference is stored if the particle crosses a sensitive region of the detector. This approximation is quite good: the presence of a track reference does not correspond to the presence of a cluster mainly for tracks with high pseudorapidity that cannot produce a signal over the threshold. Thus, the presence of at least one track

reference in each SPD layer is required. A two-dimensional histograms is filled for each reconstructable particle. The ratio between the histogram of the reconstructable particles and the reconstructed particles is the correction that takes into account the tracklet algorithm inefficiency

$$TC_{Eff}(\eta, z_{vtx}) = \frac{\sum_{triggVtxEvts} \#reconstructablePrimaries(\eta_{MC}, z_{MCvtx})}{\sum_{triggVtxEvts} \#reconstructedPrimaries(\eta_{MC}, z_{MCvtx})} \quad (7)$$

and represents for each bin the inverse of the algorithm efficiency.

Detector inefficiency A cluster from a primary could be missing due to the presence of dead or noisy channels (ladders, chips and pixels). This will cause a primary particle not to be reconstructed. In that case, that is the presence of dead subsection of the detector, this correction has to be added. This contribution is evaluated including in the simulation a dead channel map for the detector. As explained in Section 3, in this analysis the overall SPD inefficiency is about 13%, corresponding mainly to 15 excluded half-staves.

To evaluate this correction, it should be noticed that such a condition implies that this correction is automatically included in the one previously described: the reconstructable particles, whose definition relies on the presence of track references, is not affected by the presence of dead channels as the reconstructed particles. In Fig. 4 the effect of both the algorithm and the detector inefficiencies is shown. The dominant effect is that of the detector dead channels that also produces the asymmetry in the maps since the dead channels map in not symmetric in η.

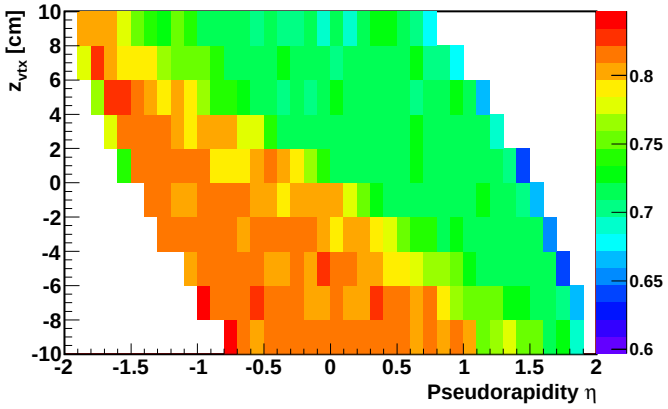

Figure 4: *Efficiency correction: these correction takes into account both the efficiency of the reconstruction algorithm and the efficiency of the detector.*

The effect of the algorithm inefficiency with the default cuts used in the reconstruction as been evaluated to be about 2%.

Geometrical acceptance This correction can be calculated once and for all for each layer and for tracklets, provided the detector geometry is fixed. The calculation is carried out selecting the **detectable** primaries, that is primaries which have reached and crossed the region in which the detector is placed. Those particles might have or might not have produced a signal in the detector according as the volume crossed is sensitive or not. The selection of the detectable primaries can be performed using the track references. As already mentioned, for each primary Monte Carlo particle a number of track references is stored during the transport through the ALICE geometry if the particle crosses the sensitive region of a detector, each of detectors being identified with a numerical label. A track reference with the numerical label = -1 is saved when the particle disappears somewhere in the geometry (detector material or empty space). A particle to be labeled as detectable for a specific detector (both SPD layers in the present case) has to satisfy one of the following:

- it has no track references at all or it has not a track reference with label equal to -1, that means it did not disappear in the ALICE geometry;
- it has a track reference with label equal to -1 and with a radius greater than the maximum radius of the track references of the detector, that means the particle disappeared after the detector;
- it has at least one track reference with radius in the range of the radii of the detector, that means the particle crossed a sensitive region of the detector considered.

As a consequence of the previous definition, particles outside the acceptance of the detector could be labeled as detectable as well, but without affecting the correction calculation since the correction will not be used outside the acceptance region of the detector. A two-dimensional histogram is filled for each detectable primary. The geometrical acceptance correction for each bin is the ratio between the histogram of detectable primaries and the histogram of reconstructable primaries

$$Acc = 1/TC_{Acc}(\eta, z_{vtx}) = \frac{\sum_{triggVtxEvts} \#detectablePrimaries(\eta_{MC}, z_{MCvtx})}{\sum_{triggVtxEvts} \#reconstructablePrimaries(\eta_{MC}, z_{MCvtx})} \quad (8)$$

In Fig. 5 the correction is shown as usual as a function of z_{MCvtx} and η_{MC} for both the SPD layers. The same map for tracklets is shown in Fig. 6. As already seen for the corrections previously shown, the pseudorapidity range covered depends on the vertex position. It can be seen in Fig. 5 that for $z_{vtx} = 0$ cm (primary vertex in the center of the detector) the main losses come from three "holes" corresponding to the three juctions between ladders: for the inner layer at η =-1.35, η =0 and η =1.35, for the outer layer at η

=-0.86, η =0 and η =0.86. For tracklets (Fig. 6) the acceptance contains the combination of all the holes in both layers.

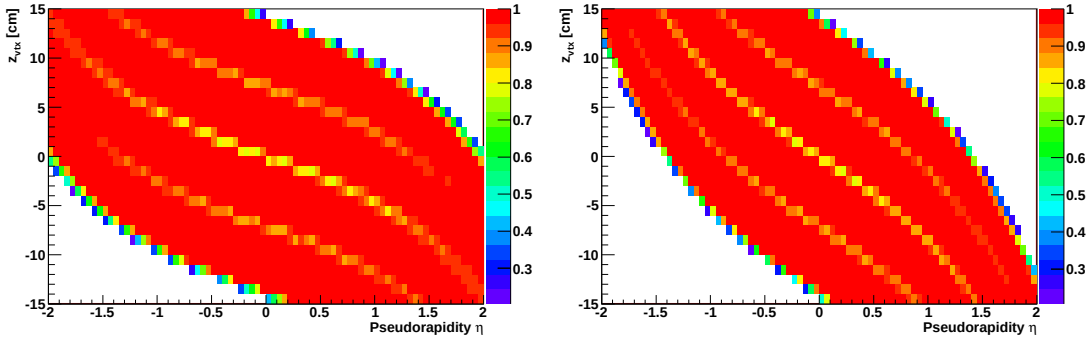

Figure 5: *Acceptance correction for the SPD inner (on the left) and outer (on the right) layer.*

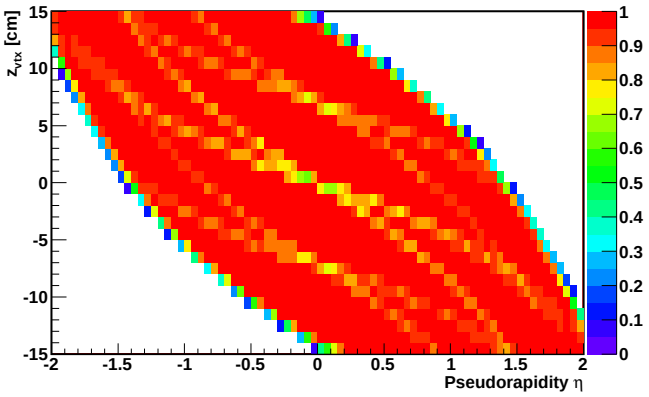

Figure 6: *Acceptance correction map for tracklets.*

The systematic error associated with this correction comes from the the error on the correction factors itself. They depend, in principle, on the model used in the generation, on the model used for particle transport and, most important, on the statistic used This last contribution gives to the weights an uncertainty of about 3%, which correspond to an error on the multiplicity itself lower than 0.3% for events at $z_{vtx} = 0cm$. The model used in the simulation on the other hand should provide a realistic p_t spectrum in order to reproduce the effect of the magnetic field on the geometrical acceptance. An estimate of the influence of the model on the correction factors can be obtained using different generators[4].

The acceptance correction map has to be taken into account at event level as well to calculate the correct normalization factors for each bin of the pseudorapidity distribution corrected for the acceptance. Indeed due the limited dimension in z of the detector and

the spread of the vertex position, not all the reconstructed events will contribute to each η bin of the corrected distribution but for each η bin a range $z_1 < z_{SPDvtx} < z_2$ of the reconstructed vertex distribution will be considered to fill the normalization histogram. For a pseudorapidity bin $\eta^{'}$ this range is defined requiring $TC_{Acc}(\eta^{'}, z) > 0$.

Particles not reaching the sensitive layers The last contribution to obtain the distribution in all the reconstructed events is that of primary particles that do not reach the outer SPD layer because they undergo secondary interactions or they decay or they have a p_t below the cut-off to reach the outer SPD layer.

The two histograms needed to calculate this correction are the one of the detectable primaries and the histogram filled for all the primaries generated in reconstructed events. The correction corresponds to the inverse fraction of primary particles that cross the SPD and is shown in Fig. 7.

$$TC_{Decays}(\eta, z_{vtx}) = \frac{\sum_{trigVtxEvts} \#Primaries(\eta_{MC}, z_{vtxMC})}{\sum_{trigVtxEvts} \#detectablePrimaries(\eta_{MC}, z_{vtxMC})} \tag{9}$$

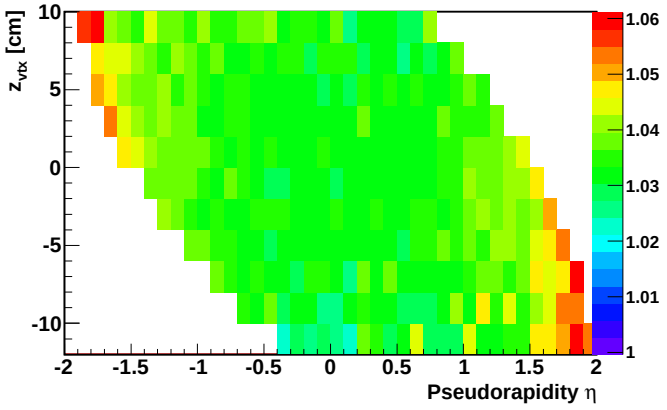

Figure 7: *Correction for particles that do not reach the SPD outer layer.*

Vertex reconstruction inefficiency and minimum bias trigger acceptance A small percentage of the triggered events could not have a vertex reconstructed so it is necessary to add at this stage the contribution of the missing events both at event level and at tracklet level.

At track level, this correction is calculated as the ratio between the primary charged particles produced by the generator in triggered events and the primary charged particle found in reconstructed events

$$TC_{Vertex}(\eta_{MC}, z_{MCvtx}) = \frac{\sum_{trigEvts} \#Primaries(\eta_{MC}, z_{MCvtx})}{\sum_{trigVtxEvts} \#Primaries(\eta_{MC}, z_{MCvtx})} \tag{10}$$

Similarly, the ratio between the primaries in all the generated events for a certain event class (inelastic or non-single diffractive) and the primaries in triggered events is the correction needed to take into account the primaries missed due to the minimum bias trigger selection.

$$TC_{Trigger}(\eta_{MC}, z_{MCvtx}) = \frac{\sum_{allEvts} \#Primaries(\eta_{MC}, z_{MCvtx})}{\sum_{trigEvts} \#Primaries(\eta_{MC}, z_{MCvtx})} \tag{11}$$

Two distinct corrections for inelastic and non-single diffractive events will be calculated. Events contributing to these two corrections are low multiplicity events in the central η region, so the correction is very low (at the level of few per mill for inelastic events) and does not show any dependence on η and z.

5.2 Event level corrections

The corrections needed at event level are calculated as a function of the reconstructed multiplicity $mult_{SPD}$ (i.e. the number of reconstructed tracklets) and the position of the Monte Carlo primary vertex z_{MCvtx}. They are the following:

- vertex reconstruction inefficiency;
- minimum bias trigger inefficiency.

These allow to calculate the normalization factors for the corresponding corrected pseudo-rapidity distributions to obtain the dN/dη distributions. To calculate them, besides the information used for track level correction calculation, the tracklet multiplicity is used.

Vertex reconstruction inefficiency The vertex reconstruction inefficiency correction is the ratio between all triggered events and all the reconstructed events in each bin

$$EC_{vertex}(mult_{SPD}, z_{MCvtx}) = \frac{\sum_{triggEvts} \#events(mult_{SPD}, z_{MCvtx})}{\sum_{triggVtxEvts} \#events(mult_{SPD}, z_{MCvtx})} \tag{12}$$

In Fig. 8 the correction is shown. It is equal to one everywhere by construction and zero in the zero-multiplicity bin since events with zero tracklet multiplicity are not considered in the sample of reconstructed events.

Indeed, even if events with zero tracklet multiplicity might have a reconstructed vertex (1%), it has been verified that this vertex is not reliable at all, as it can differ from the Monte Carlo vertex several centimeters.

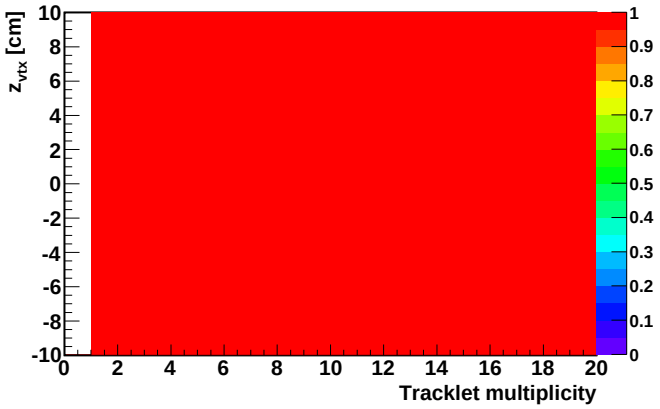

Figure 8: *Correction for vertex finding inefficiency at event level.*

Minimum bias trigger inefficiency The trigger efficiency correction is calculated as the ratio between two-dimensional matrices: one filled for all the events generated in a certain event class and the other filled for all triggered events

$$EC_{trigger}(mult_{SPD}, z_{MCvtx}) = \frac{\sum_{allEvtsevClass} \#events_{evtClass}(mult_{SPD}, z_{MCvtx})}{\sum_{triggEvts} \#events(mult_{SPD}, z_{MCvtx})} \quad (13)$$

In Fig. 9 the correction is shown for inelastic and non-single diffractive events. For inelastic events it is equal to one for $mult_{SPD} > 0$ and greater than one in the zero-multiplicity bin since it has to add inelastic events that have not been triggered. The correction for non-single diffractive events is less than one since it has to subtract single diffractive events from the selected sample.

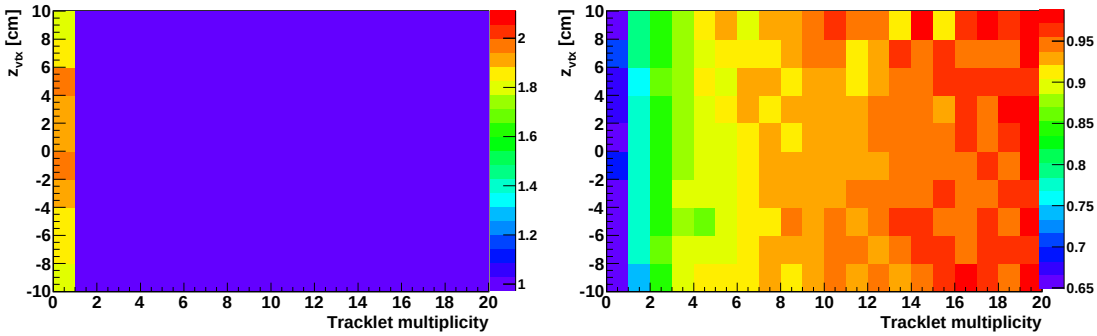

Figure 9: *Correction for the minimum bias trigger selection inefficiency for inelastic events (left panel) and for non-single diffractive events (right panel).*

6 Corrected distributions

In this section the corrections to the pseudorapidity density distribution previously described will be applied to the reconstructed Monte Carlo data. Fig. 10 shows the reconstructed and the Monte Carlo primary charged particle distributions.

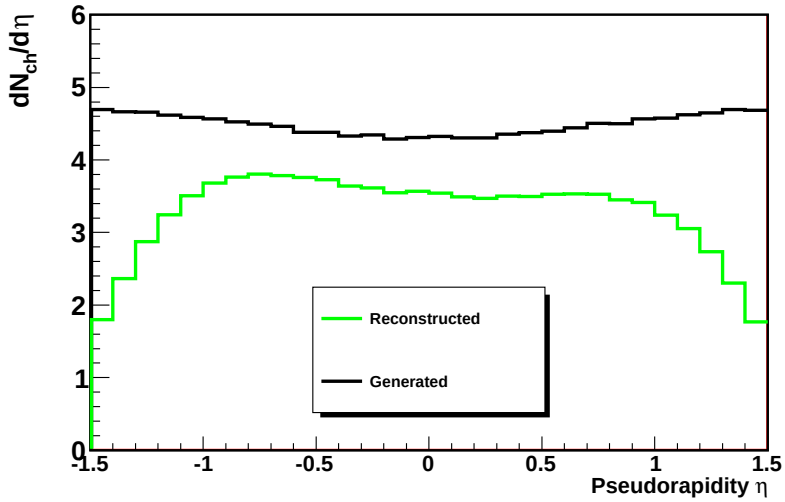

Figure 10: *dN/dη distribution reconstructed with the tracklet method (green histogram) and Monte Carlo distribution for primary charged particles (black histogram).*

Events contributing to this distribution are the reconstructed events. Here the effect of the detector acceptance can be seen in particular for $|\eta| > 1$: this effect will be corrected at event level with a proper normalization factor that takes into accout only events that contribute to each η bin.

The tracklet data matrix will be multiplied for each correction, adding one correction at a time to show the effect step by step.

$$tracklets(\eta, z_{vtx}) * \prod_i TLC_i(\eta, z_{vtx}) \tag{14}$$

The projections on η axis are normalized as follows:

- with the number of reconstructed events for each bin, if the distribution is not corrected for acceptance;
- with an histograms taking into account events that contribute to each pseudorapidity bin according to the acceptance correction.

In Fig. 11 the results applying one correction at a time is shown. The distribution after background subtraction has a small fraction of tracklets less than the reconstructed as ex-

pected. The efficiency corrections is quite high and makes the distribution symmetric. To correct for the acceptance, the track level map is not enough: a normalization histogram has to be filled as illustrated previously. Looking at the distribution corrected also for acceptance, the effect of the proper normalization is noticeable for $|\eta| > 1$. The higher distribution is the distribution in the reconstructed events.

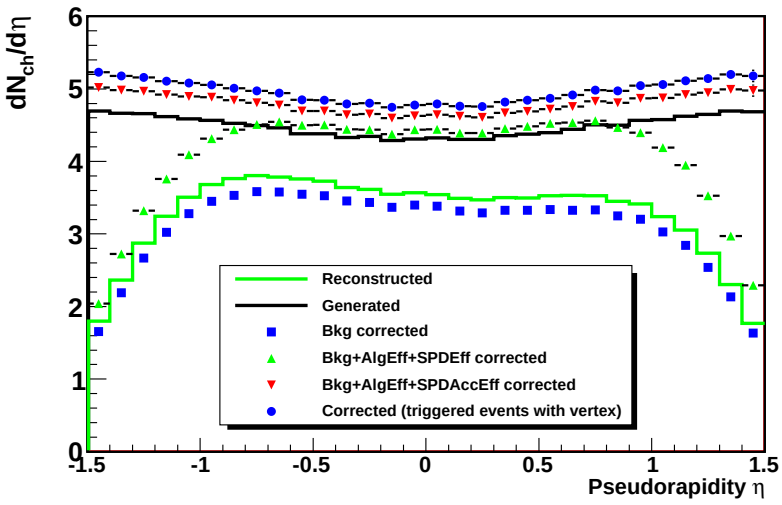

Figure 11: *dN/dη distribution reconstructed with the tracklet method (green histogram) and Monte Carlo distribution for primary charged particles (black histogram). All the other curves represent the corrected distribution adding one correction at a time and normalizing the distributions properly.*

Now two corrections are need both at track and at event level to obtain the distribution in all the triggered event first and in all events for the two event classes. The vertex correction is unity at event level and is less than one per mill at track level. To obtain the normalization histogram and afterwards to apply the trigger correction at event level, the vertex distribution of triggered events has to be known: the issue is that triggered events with zero tracklet reconstructed do not have a vertex. So it is needed to known how triggered events in the zero multiplicity bin are distributed in vertex. For this purpose Monte Carlo information can be used, or assuming the vertex distribution to be independent of multiplicity, the distribution can be inferred from data. The only information available from data is the vertex distribution of reconstructed events, so that the fraction of reconstructed events for each vertex bin can be calculated. The triggered events with zero tracklet multiplicity will be distributed in vertex bins using these fractions and correcting these fractions using the Monte Carlo: events used to calculate the fractions are not only triggered but also have a vertex and this additional condition can bias the distribution. The correction will take into account how the triggered events with zero

multiplicity should be distributed with respect to all the reconstructed events. These correction factors are very small. In Fig. 12 the three distributions for inelastic events, applying these corrections at track and event level are shown. In Fig. 13 the final results are compared to the Monte Carlo distribution for each of the two event classes (left panel), while in the central and righ panel of the same figure the corresponding ratios are shown.

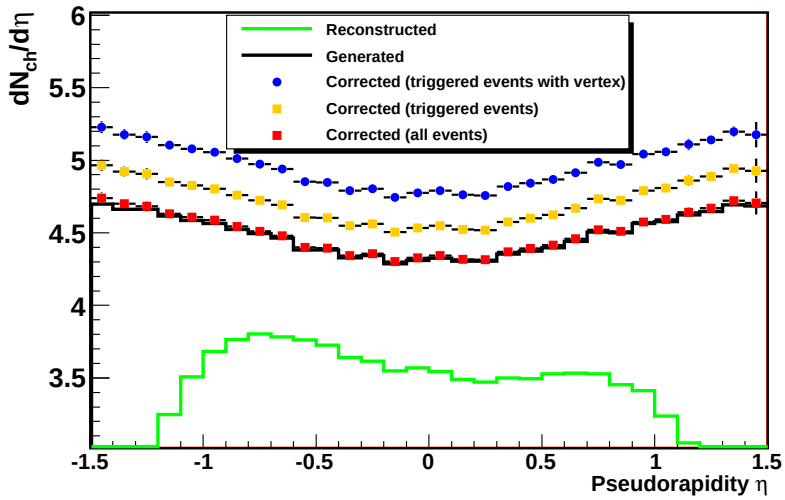

Figure 12: *dN/dη distribution reconstructed with the tracklet method (green histogram) and Monte Carlo distribution for primary charged particles (black histogram). All the other curves represent the corrected distribution adding one correction at a time.*

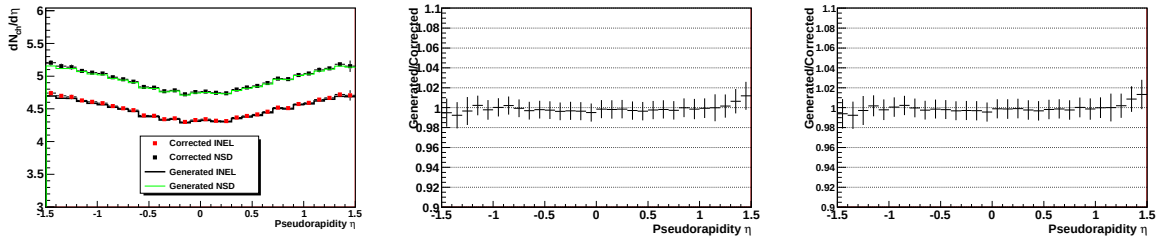

Figure 13: *dN/dη distribution corrected for inelastic and non-single diffractive events (left panel). The ratio between the Monte Carlo and the corrected distribution are shown for all inelastic (central panel) and non-single diffractive (right panel) events separately.*

A verification of the method can be performed using the same sample both to calculate corrections and to fill the data matrices: only primary particles are processed (the background correction is unity) and the Monte Carlo values for the pseudorapidity and the vertex position are used. The Monte Carlo distribution in the SPD acceptance has to be obtained if the method is correct. In Fig. 14 the ratio between the generated distribution

in the SPD acceptance and the corrected distribution is shown.

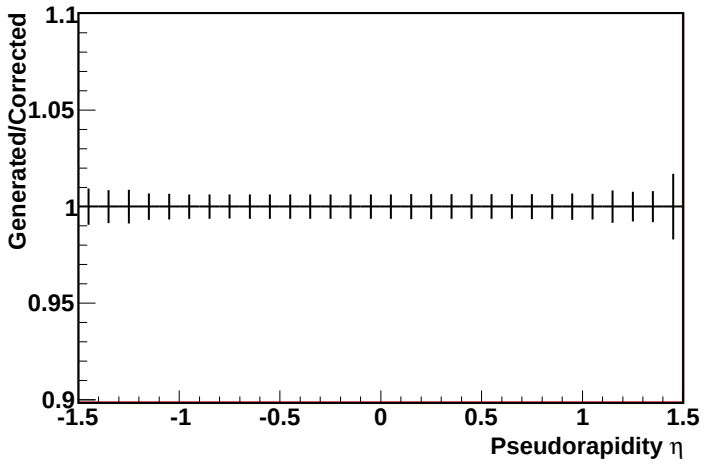

Figure 14: *Ratio between the Monte Carlo $dN_{ch}/d\eta$ distribution in inelastic events in the SPD acceptance and the corrected distribution obtained processing only primary particles and using the Monte Carlo values for the pseudorapidity and the primary vertex. The ratio is unity in the SPD acceptance that confirms that the method is correct and takes into accout all the contributions.*

7 Summary and conclusions

An analysis method for the measurement of the pseudorapidity density distribution of charged particles in proton-proton collisions has been developed. The method is based entirely on the information coming from the Silicon Pixel Detector in the inner tracking system. It takes into account all the effects coming from detector and reconstruction efficiencies: the corresponding correction factors have been estimated and applied using the official (AliRoot) simulation and reconstruction framework and Monte Carlo productions from the PDC09. Details of the method and its main results, which are compatible with those provided by the alternative method in Ref. [2], are shown in this note. The corresponding software has been integrated in the PWG2 directory of the AliRoot package.

References

[1] K. Aamodt *et al.*, JINST **3** (2008) S08002.

[2] J. F. Grosse-Oetringhaus, CERN-THESIS-2009-033.

[3] ALICE ITS Technical Design Report, CERN/LHCC 99-12, 1999.

[4] T. Virgili *et al.*, ALICE Internal Note, ALICE-INT-2002-043.

[5] T. Virgili, ALICE Internal Note, ALICE-INT-2006-013.

[6] D. Elia *et al.*, ALICE Internal Note, ALICE-INT-2009-021.

[7] A. Dainese and M. Masera, ALICE Internal Note, ALICE-INT-2003-027.

[8] E. Bruna *et al.*, ALICE Internal Note, ALICE-INT-2009-018.

[9] B. B. Back et al., PHOBOS Collaboration, Phys. Rev. Lett. **85** (2000) 3100.

[10] J. Conrad *et al.*, ALICE Internal Note, ALICE-INT-2005-025.

[11] ALICE Physics Performance Report, Volume II, J. Phys. G: Nucl. Part. Phys. 32, (2006), 1295-2040.

[12] ALICE Physics Performance Report, Volume I, J. Phys. G: Nucl. Part. Phys. 30, (2004), 1517-1763.